New Mexico Geological Society

Downloaded from: https://nmgs.nmt.edu/publications/guidebooks/58

Comments on the geology, petrography, and chemistry within the resurgent dome area, Valles Caldera, New Mexico

Fraser Goff, Richard G. Warren, Cathy J. Goff, Jennifer Whiteis, K, Emily uk, and Dale Counce
2007, pp. 354-366. https://doi.org/10.56577/FFC-58.354

in:

Geology of the Jemez Region II, Kues, Barry S., Kelley, Shari A., Lueth, Virgil W.; [eds.], New Mexico Geological Society 58 th Annual Fall Field Conference Guidebook, 499 p. https://doi.org/10.56577/FFC-58

This is one of many related papers that were included in the 2007 NMGS Fall Field Conference Guidebook.

Annual NMGS Fall Field Conference Guidebooks

Every fall since 1950, the New Mexico Geological Society (NMGS) has held an annual Fall Field Conference that explores some region of New Mexico (or surrounding states). Always well attended, these conferences provide a guidebook to participants. Besides detailed road logs, the guidebooks contain many well written, edited, and peer-reviewed geoscience papers. These books have set the national standard for geologic guidebooks and are an essential geologic reference for anyone working in or around New Mexico.

Free Downloads

NMGS has decided to make peer-reviewed papers from our Fall Field Conference guidebooks available for free download. This is in keeping with our mission of promoting interest, research, and cooperation regarding geology in New Mexico. However, guidebook sales represent a significant proportion of our operating budget. Therefore, only *research papers* are available for download. *Road logs*, *mini-papers*, and other selected content are available only in print for recent guidebooks.

Copyright Information

Publications of the New Mexico Geological Society, printed and electronic, are protected by the copyright laws of the United States. No material from the NMGS website, or printed and electronic publications, may be reprinted or redistributed without NMGS permission. Contact us for permission to reprint portions of any of our publications.

One printed copy of any materials from the NMGS website or our print and electronic publications may be made for individual use without our permission. Teachers and students may make unlimited copies for educational use. Any other use of these materials requires explicit permission.

This page is intentionally left blank to maintain order of facing pages.

New Mexico Geological Society Guidebook, 58th Field Conference, Geology of the Jemez Mountains Region II, 2007, p. 354-366.

COMMENTS ON THE GEOLOGY, PETROGRAPHY, AND CHEMISTRY OF ROCKS WITHIN THE RESURGENT DOME AREA, VALLES CALDERA, NEW MEXICO

FRASER GOFF[1], RICHARD G. WARREN[2], CATHY J. GOFF[3], JENNIFER WHITEIS[4], EMILY KLUK[5], AND DALE COUNCE[5]

[1]Department of Earth and Planetary Sciences, University of New Mexico, Albuquerque, NM 87131
[2]Comprehensive Volcanic Petrographics, 2622 H Rd., Grand Junction, CO 81506
[3]Geologic Consultant, 5515 Quemazon, Los Alamos, NM 87544
[4]New Mexico Bureau of Geology and Mineral Resources, 801 Leroy Place, Socorro, NM 87801
[5]Earth and Environmental Sciences Division, Los Alamos National Laboratory, Los Alamos, NM 87544

ABSTRACT — We briefly describe the geology, petrography and chemistry of rocks from the resurgent dome of Valles caldera using recently published 1:24,000 geologic mapping, supported by thin section examinations and chemical analyses. Eruptive rocks consist of lavas and tuffs of rhyolite to high-silica rhyolite. A 110 m-thick section of densely welded ignimbrite exposed along Redondo Border apparently correlates with the two uppermost stratigraphic units of the Tshirege Member, Bandelier Tuff on the Pajarito Plateau east of the caldera. Caldera collapse breccias consist of Quaternary Otowi Member of Bandelier Tuff, Miocene to Pliocene volcanic rocks, Permian to Miocene clastic rocks, and Pennsylvanian limestone. The age, petrography and chemistry of the volcanic collapse breccias resemble those described for the Tschicoma and Paliza Canyon Formations in the surrounding Jemez Mountains. Early caldera-fill debris flow, fluvial, and lacustrine sediments are derived from the above lithologies but tend to have higher silica and less total alkalis than source rocks due to chemical weathering and hydrothermal alteration. Altered rocks and veins are silica-rich and alkali-poor, and generally contain enhanced iron, sulfur and arsenic values. Rhyolite vitrophyre from ignimbrite just northwest of Cerro Seco, one of the post-collapse ring fracture domes, has chemistry very comparable to Seco rhyolite lava. Thus, we interpret these pyroclastic deposits as the initial eruptions that eventually culminated with Cerro Seco dome.

INTRODUCTION

During the past several years, the geology of the Valles caldera (Fig. 1) has been mapped at 1:24,000 scale as part of the joint U.S. Geological Survey-New Mexico Bureau of Geology and Mineral Resources State Map Program. Roughly 20 quadrangles in the Jemez Mountains have been completed or are nearing completion. The resurgent dome of Valles caldera (Fig. 2) lies within the Bland, Redondo Peak, Valle San Antonio, and Valle Toledo quadrangles (Goff et al., 2005a, b, 2006; Gardner et al., 2006). To complement recent geoscientific studies occurring within Valles caldera and to provide background information for Day 2 of the 2007 New Mexico Geological Society field conference, we briefly describe selected aspects of the geology, petrography, and chemistry of resurgent dome rocks within the caldera.

BACKGROUND GEOLOGY

Valles caldera (Fig. 1) formed at 1.25 Ma during eruption of approximately 300 km^3 of the Tshirege Member, Bandelier Tuff (Smith et al., 1970; Phillips et al., in press). The caldera collapsed more or less at the same time as the Tshirege ignimbrites erupted. As the caldera collapsed, landslide blocks (megabreccias) fell off the caldera wall and were incorporated into the intracaldera ignimbrites (e.g., Goff et al., 2005a). Drill hole and gravity data show that the amount of collapse was significant (Nielson and Hulen, 1984; Nowell, 1996). More than 1100 m of Tshirege ignimbrite have been penetrated by wells in the Redondo Creek graben of the Valles resurgent dome. After the caldera formed several events began to occur almost simultaneously. First a lake formed and sediments accumulated in the caldera depression. Second, small-volume rhyolite tuffs and lavas erupted and are interbedded with early caldera-fill sediments. Third, the resurgent dome began to rise due to continued magma pressure from below (Smith and Bailey, 1968). The resurgent dome rose out of a lake to a height of approximately 1000 m (1 km) above the surrounding valleys. As it rose, more rhyolite eruptions occurred and sediments on the resurgent dome were shed into the adjacent caldera moat. Recent high precision $^{40}Ar/^{39}Ar$ dating shows that

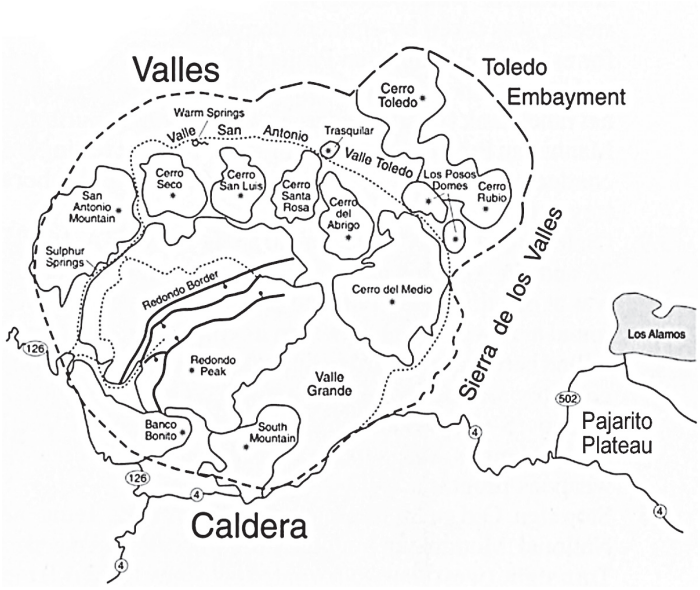

FIGURE 1. Location map of the Valles caldera, New Mexico.

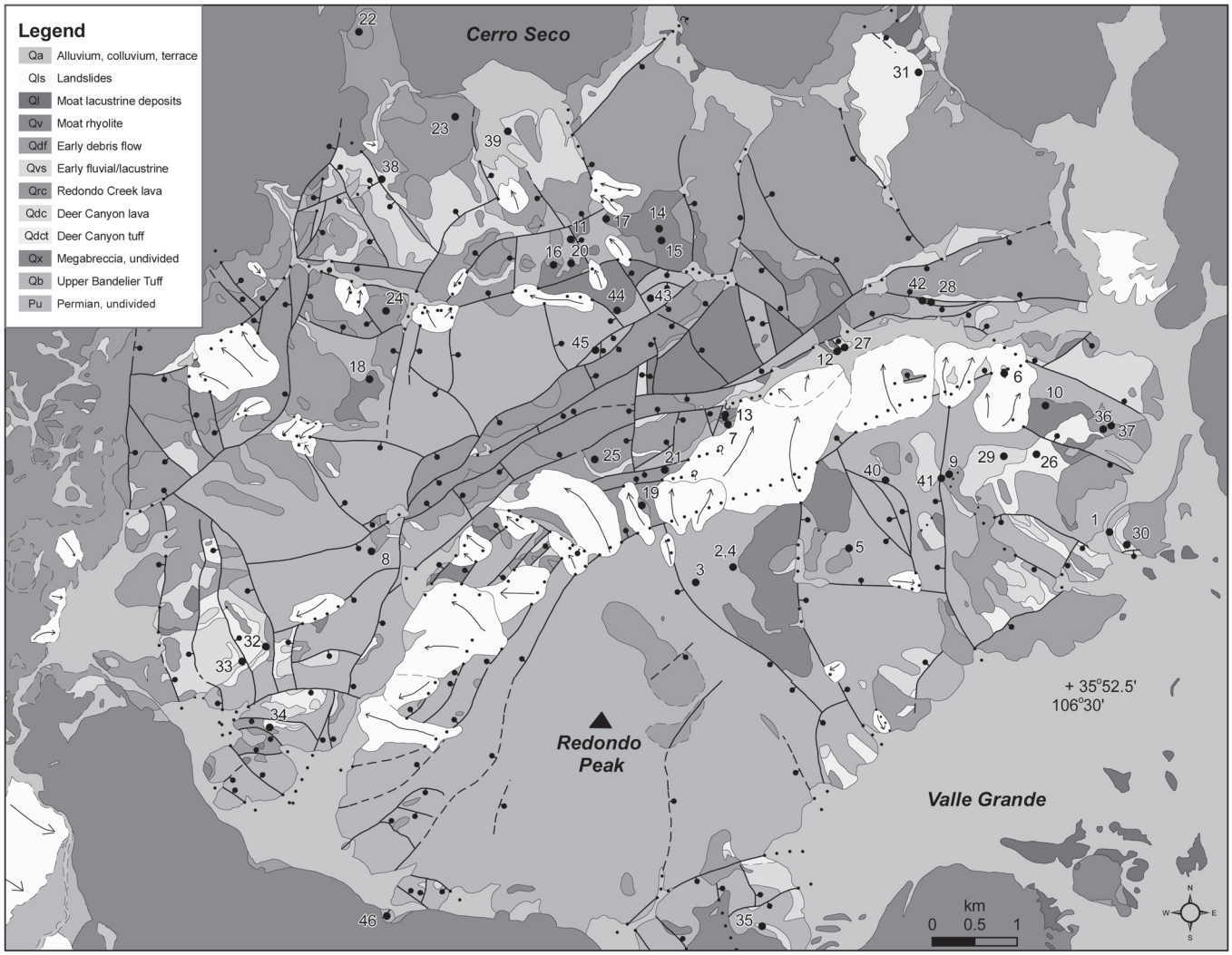

FIGURE 2. Generalized geologic map of the resurgent dome of Valles caldera and surrounding caldera moat, compiled and simplified from the following 1:24,000 maps: Bland (Goff et al., 2005b), Jemez Springs (Kelley et al., 2003), Redondo Peak (Goff et al., 2005a), Seven Springs (Kelley et al., 2004), Valle San Antonio (Goff et al., 2006), and Valle Toledo (Gardner et al., 2006). Numbers on map are keyed to sample locations in Table 1. Arrows on landslides indicate direction of movement. Ball and bar on faults indicates down-thrown side. For color version of this map, see Plate 13 on page 143.

resurgence happened within a few tens of thousands of years of caldera formation (Phillips, 2004; Phillips et al., in press). After resurgence was complete or mostly complete, the caldera moat began to fill with a series of rhyolite domes, flows, and pyroclastic deposits (Valles Grande Member and El Cajete Series) erupted from the caldera ring fracture zone. Subsequently, the moat filled with additional fluvial deposits and lacustrine sequences (Smith et al., 1970; Rogers et al., 1996). Hydrothermal activity began as soon as the caldera formed and caused widespread alteration, especially on and within the resurgent dome (Goff and Gardner, 1994). The present geothermal system (roughly 300°C) is merely the youngest manifestation of a long-lived hydrothermal system (WoldeGabriel and Goff, 1992).

ANALYTICAL METHODS

Major and trace elements for selected rock samples (Appendix 1) were analyzed using an automated Rigaku wavelength-dispersive X-ray fluorescence (XRF) spectrometer. Samples were first crushed and homogenized in 5-10 g portions in a tungsten-carbide ballmill. Sample splits were heated at 110°C for 4 hrs, and then allowed to equilibrate at ambient laboratory conditions for 12 hrs. To obtain the fusion disks, one-gram splits were mixed with 9 g of lithium tetraborate flux and initially heated in a muffle furnace for 45 min at 1100°C, followed by a second heating for 1 hr at 1150°C. Additional one-gram splits were heated at 1000°C to obtain the Loss on Ignition (LOI) measurements to be used in the data reduction program. Elemental concentrations were calculated by comparing X-ray intensities for the samples to those for 21 standards of known composition using "consensus values" from Govindaraju (1994). Intensities were reduced using a fundamental parameters program for matrix corrections (Criss, 1979).

Additional 0.25 g splits of the rock powders were mixed in a cocktail consisting of 2.0 ml HNO_3, 3.5 ml HCl, and 1.5 ml HF, heated in a microwave oven for about 10 min, and the resulting solution adjusted to 50 ml with deionized water. Analyses

of selected trace metals were done by a combination of atomic adsorption spectroscopies (graphite furnace, hydride generator, inductively coupled plasma) and ion chromatography (Goff et al., 2002; table 3). Besides providing some additional analyses for trace elements not obtained by XRF methods, the wet chemical analyses provide some checks on the precision of XRF values for P_2O_5, Rb, and Cr.

RESURGENT DOME ROCKS

Tshirege Member of Bandelier Tuff

The Tshirege Member (commonly referred to as the upper Bandelier Tuff; Fig. 3) is the dominant rock type on the Valles resurgent dome and has a maximum thickness of 1155 m near the head of Redondo Creek (Nielson and Hulen, 1984). The most recent date on the Tshirege is 1.256 ± 0.010 Ma (Phillips et al., in press). Because it is so thick, most of the Tshirege is not exposed and can only be studied from cuttings and cores (Hulen and Nielson, 1986; Hulen et al., 1991; Goff and Gardner, 1994; Warren et al., 2007). Intracaldera Tshirege is a classic ash-flow tuff (ignimbrite) that is welded to densely welded, usually displaying a near-horizontal fabric due to vertical variations in welding, devitrification, fiamme, and alteration. The color is usually gray to pale tan and pink. Phenocrysts consist almost entirely of abundant sanidine/anorthoclase and quartz. Sparse to trace clinopyroxene, orthopyroxene, fayalite, opaque oxides, apatite, and chevkenite are also found (Caress, 1996). Warren et al. (2007) provide average values for phenocrysts by subunit. The sanidine is often chatoyant blue, while the pyroxene and opaque minerals are usually oxidized, making them difficult to see with a hand lens. Lithic content is highly variable but most exposures of Tshirege will reveal some lithics. The lithic population is mostly composed of precaldera volcanic rocks and sandstones. Near megabreccia blocks, lithics are generally abundant, some >0.2 m in length.

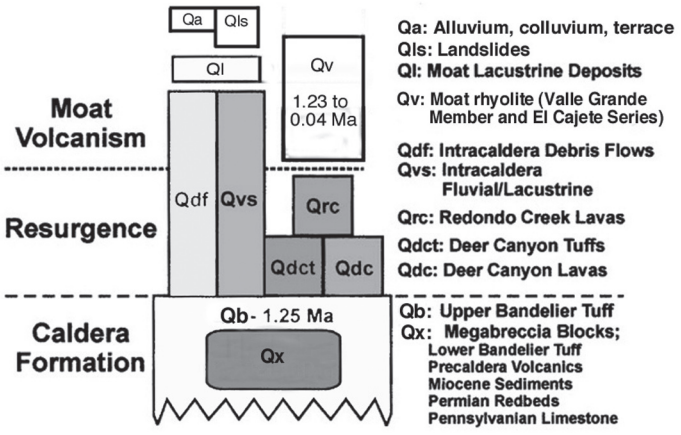

FIGURE 3. Generalized stratigraphy of the resurgent dome and vicinity adapted from Self et al. (1988), Phillips et al. (in press) and Chipera et al (in press). Unit labels correspond to those in the legend of Figure 2**.** Goff et al. (2006) provided a comprehensive correlation chart for all units discussed in this report.

Because of substantial uplift during resurgence, intracaldera Tshirege usually forms outcrops of broken plates, particularly on the Redondo Peak block. Unbroken or unfaulted outcrops are usually not continuous.

Where exposed, the top of the Tshirege is white from alteration and weathering, and highly vesicular from presence of nonwelded pumice. The vesicular top is usually less than 1 m thick. Where stratigraphic context is preserved, a black vitrophyre usually occurs about 1.5 to 3 m below the top of the unit. The vitrophyre often has distinctly visible clinopyroxene, as well as sanidine and quartz, and fiamme up to 20 cm long. However, many other vitrophyre horizons occur within the intracaldera Tshirege section.

Thin sections of the Tshirege show classic eutaxitic texture consisting of glass shards, pumice, crystals, and lithics in a banded to massive, welded to densely welded matrix (Ross and Smith, 1961). The glass, if fresh, is commonly black to brown to orange-brown. Both broken and unbroken crystals occur. Sanidine crystals are commonly full of melt inclusions. Unbroken quartz is commonly embayed as if out of equilibrium. Pyroxene crystals vary from <0.01 to 0.3 mm and opaque oxides are up to 0.05 mm. Crystal clots of feldspar-pyroxene are sparse. Devitrified samples are much more common than vitric. When devitrified, the pumice and glass contain tiny, low-birefringent minerals (primarily a silica phase and alkali feldspar) and vesicles are filled with tridymite. Pyroxene and opaque oxides are difficult to find, recognized mostly as pseudomorphs.

The intracaldera vitrophyre near the top of the Tshirege section is noteworthy because it contains abundant clinopyroxene up to 2.5 mm long and 0.5 mm wide. The clinopyroxene is yellow green, slightly pleochroic, and partly reacted to brownish amorphous Fe-oxides and clay in most thin sections. The intracaldera vitrophyre also contains clots of feldspar (some of which is plagioclase) and pyroxene up to 2 mm long.

Chemically, the Tshirege Member exposed on the resurgent dome is rhyolite to high-silica rhyolite (>75 wt-% SiO_2) with 8 to 10 wt-% $Na_2O + K_2O$ (Appendix 1; Fig. 4). Most samples have relatively high contents of TiO_2 (>0.2 wt-%) and relatively high Ba, Rb, Sr, and Zr. Warren et al. (2007) provide average values for each subunit.

Outside the caldera, the Tshirege forms a sequence of recognizable sheets or flow units (Smith and Bailey, 1966). The most recent discussions of unit distinctions are summarized by Gardner et al. (2001) and Lewis et al. (2002). Their uppermost Tshirege unit is named Unit 4. Unit 4 has highly variable chemical, physical, and spatial properties, but has been generally broken into a lower subunit (4L) and an upper subunit (4U) that correspond to Units 4 and 5 of Warren et al. (1997) and generally with units E and F of Rogers (1995). Gardner et al. (2001) pointed out that subunit 4L *sometimes* has unusually high TiO_2 contents (>0.3 wt-%) and that subunit 4U is generally clot-rich and moderately to densely welded. The clots contain feldspar-pyroxene-amphibole. At least some of the feldspar is plagioclase. TiO_2 contents of unit 4U are generally between 0.2 and 0.3 wt-%. Gardner et al. (2001) also pointed out that Unit 4 ignimbrites generally contain higher Ba, Rb, Sr, and Zr than lower flow units. We have also noticed that thin sections of welded unit 4U contain pleochroic clinopy-

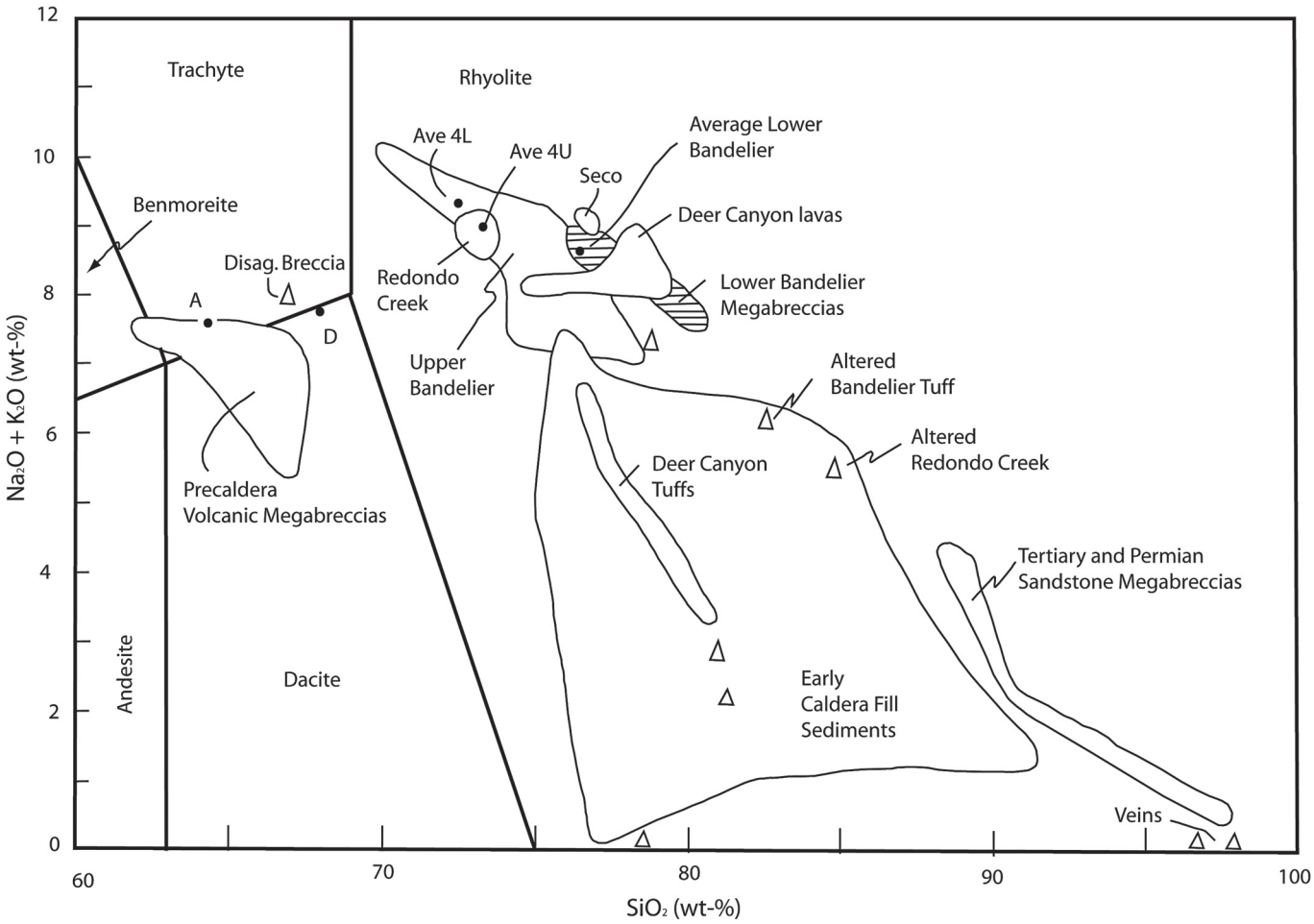

FIGURE 4. Plot of total alkalis ($Na_2O + K_2O$) versus SiO_2 for rocks of the Valles caldera resurgent dome and vicinity. The left half of the diagram is a Le Bas plot (Le Bas et al., 1986). All data are normalized LOI-free to 100% from analyses in Appendix 1. The fields enclose related groups of rocks. Symbols: A = Paliza Canyon andesite, D = Tschicoma dacite, 4L, 4U = average Units 4L and 4U of the Upper Bandelier Tuff, triangles = veins, gouge, breccias, and highly altered rocks.

roxene of similar size and optical properties to those found in the uppermost intracaldera vitrophyre. Histograms in Warren et al. (2007) illustrate and quantify these observations.

Doell et al. (1968) mentioned that the uppermost Bandelier Tuff unit on the Pajarito Plateau (east of the caldera) is found throughout the resurgent dome but they provided no data to support their statement. We have analyzed seven samples from an 80 m section of Tshirege Member exposed on the east margin of Redondo Border (Appendix 1; Fig. 2, site 8). Significantly, samples from the lower part of this section have TiO_2 greater than 0.3 wt-%, similar to Unit 4L, whereas samples from the upper part of the section contain 0.2 to 0.3 wt-% TiO_2, similar to Unit 4U (Fig. 5). For samples in this section, there also seems to be a positive correlation from top to bottom of Ba and TiO_2. The lower samples have >500 ppm Ba, whereas the upper samples have 300 to 400 ppm Ba. Interestingly, the chemistry of these samples does not precisely mirror the flow unit boundary that we observed in the section. Judging from the chemistry of the other samples we have taken, it appears that most of the Tshirege on the resurgent dome belongs to Unit 4U, supporting the general statement of Doell et al. (1968).

Warren et al. (2007) show that Tshirege units on the Pajarito Plateau correlate with surface and subsurface intracaldera Tshirege units on the basis of petrography, mineral chemistry, and rock chemistry. This is the first time that such precise correlations have been compared among sections of Bandelier Tuff in the interior and exterior caldera environments and the resulting information may prove useful for future study of eruption processes in sequential magma batches from the Bandelier chamber.

Caldera collapse breccias (megabreccias)

Lipman (1976) defined caldera collapse breccias as large, intact blocks that slide off the structural wall of a caldera and into the caldera depression as the caldera is formed. They are incorporated into the intracaldera ash-flow tuffs (Fig. 3). According to Lipman (1976, 2000), most of the collapse breccias occur near the bottom of the ash-flow tuff sequence, indicating that most of the sliding occurs near the beginning of the caldera-forming eruptions. However, we have found significant quantities of collapse breccias at the top of the ash flow sequence (e.g., Goff et al., 2006). Some of the breccias form small hills above the sur-

rounding tuff, suggesting they were never completely submerged in the tuff. The types of rocks comprising the breccias are somewhat correlated with the type of basement underlying the caldera. Thus, precaldera volcanic rocks are the most common collapse breccias in the north and east of the resurgent dome, whereas Permian rocks are most common in the south and west. Several breccia types were chemically analyzed (Appendix 1).

Collapse breccias composed of Otowi Member of Bandelier Tuff (commonly referred to as lower Bandelier Tuff) are massive to ruptured (megabreccia breccias!). Most show some type of hydrothermal alteration. Tuff within the breccias is usually characterized by silicification of the matrix. Chatoyant sanidine and quartz phenocrysts are prominent. Fiamme are well expressed, especially on weathered surfaces. Rock colors are dominantly brown to reddish brown but gray, pale blue, pale green and white colors are common. A sample from a large Otowi collapse breccia on the west side of the resurgent dome was dated at 1.68 Ma by Phillips (2004, average of two dates). This age compares favorably to those obtained on in-place Otowi Member samples from outside the caldera (Izett and Obradovich, 1994; Spell et al., 1996). Silicified Amalia Tuff (about 26 Ma), such as found as cobbles in sediments of the Abiquiu Formation and the Chama-El Rito member of the Tesuque Formation north of the caldera, resembles silicified Otowi, but the latter tends to have smaller and more abundant phenocrysts.

In thin section, samples of Otowi Member have typical eutaxitic texture but show extensive silicification. Spherulitic shapes are common in the collapsed pumice fragments. Pyroxene and opaque oxides are completely destroyed. Small lithic fragments are common. Chemically, these samples are high-silica rhyolites but have higher SiO_2, lower TiO_2 and Al_2O_3, and lower Ba, Sr, and Zr than samples from Tshirege Units 4L and 4U (Appendix 1). Total alkalis within samples of Otowi collapse breccia are roughly similar to samples of the Tshirege Member (Fig. 4). Samples of Otowi collapse breccia are more or less similar in chemistry to the average composition of Otowi ash-flows in a stratigraphic section from a well on the Pajarito Plateau (Gardner et al., 2001).

Precaldera volcanic rocks are well represented in the collapse breccias (e.g., Goff et al., 2006). They consist of lava flows, flow breccias, lithic tuffs, and debris flow deposits of predominantly andesite to dacite from both the Paliza Canyon and Tschicoma Formations (Bailey et al., 1969). Basalt and aphyric rhyolite are occasionally found as blocks and cobbles in the debris flow deposits. Low temperature alteration to illite-chlorite grade is relatively common. Some blocks show silicification and pink to red oxidation. Fractures are commonly injected with Bandelier ignimbrite. Two samples were dated (Phillips, 2004): a dacite in the gigantic collapse breccia 2.5 km northeast of Redondo Peak (2.004 ± 0.018 Ma, see Fig. 2) and a dacitic tuff in Redondo Border (8.205 ± 0.083 Ma, near site 44, Fig. 2). Most samples of the intermediate composition rocks contain plagioclase, augite, and hypersthene. The more evolved rocks may also contain hornblende and/or biotite. Potassium feldspar is uncommon. We did not observe phenocrystic quartz in the dacites. Chemically, the andesites and dacites cross the boundary between calc-alkaline and alkaline compositions on a La Bas plot (Fig. 4) and some rocks could be called benmoreite and trachyte. This characteristic was previously noted by WoldeGabriel et al. (2001) and Wolff et al. (2005). In all other respects, chemical compositions of andesites and dacites resemble those of Paliza Canyon and Tschicoma formations presented by Gardner et al. (1986).

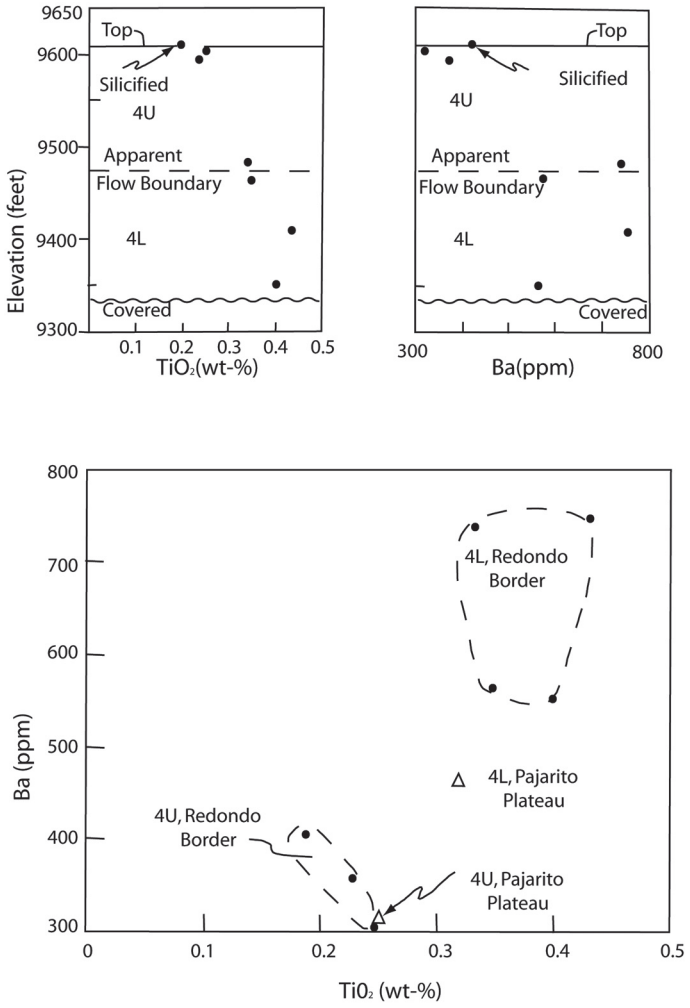

FIGURE 5. **Upper:** Plots of elevation (feet) versus TiO_2 (wt-%) and Ba (ppm) for a section of intracaldera Tshirege Member, Bandelier Tuff exposed along Redondo Border (site 8, Fig. 2 and Appendix 1). **Lower:** Plot of Ba (ppm) versus TiO_2 (wt-%) for rocks from the Tshirege section at site 8 (Fig.2), compared with average Tshirege Unit 4L and Unit 4U on the Pajarito Plateau.

Tertiary to Permian clastic rocks are also quite common as collapse breccias on the resurgent dome, mostly as massive to bedded sandstone and shale. Quartz is the dominant detrital component. Feldspar and hematite cement is most common in Permian samples. As a group, these older clastic rocks are silica-rich and alkali-poor compared with all volcanic rocks (Fig. 4). We found one zone containing relatively abundant, Paleozoic limestone collapse breccias on the western side of the resurgent dome but did not analyze them. Kues and Goff (2007) describe the paleontology of several limestone blocks near Sulphur Springs.

Early rhyolite eruptions

The first eruptions to follow collapse of Valles caldera were a series of small-volume rhyolite tuffs and lavas named the Deer Canyon Member (Fig. 4; Bailey et al., 1969). The most recent $^{40}Ar/^{39}Ar$ work yields a range of 1.229 to 1.283 Ma for the Deer Canyon (Phillips et al., in press). The tuffs consist primarily of lithic fall or hydromagmatic surge deposits. The surge deposits commonly contain accretionary lapilli. One Deer Canyon ignimbrite that was previously interpreted as part of the younger Valles Grande Member tuffs was erupted on the north flank of the resurgent dome (Fig. 2). Generally speaking, Deer Canyon lavas overlie these tuffs but at a few locations the lavas rest on Bandelier Tuff or are interbedded within caldera-fill sedimentary rocks (described below). At several locations the lavas are sandwiched between Deer Canyon tuffs. Lava flows erupted on the eastern side of the resurgent dome are fine grained and nearly aphyric whereas those on the western resurgent dome are extremely porphyritic, suggesting there were two magma reservoirs that erupted at virtually the same time. On the eastern side of the resurgent dome we found two locations where the rhyolite has pillow shapes indicating probable flow into a lake. Most Deer Canyon rocks, whether tuffs or lavas, show moderate to severe, low-temperature hydrothermal alteration due in part to their eruption into the first Valles caldera lake (Chipera et al., in press; 2007).

In thin section, Deer Canyon tuffs contain a mixture of ash, pumice, crystal and lithic fragments. The ignimbrite has relict eutaxitic texture. Lithic fragments are mostly precaldera volcanics, massive to spheroidal rhyolite, Bandelier Tuff, and what appears to be chert. The crystals are quartz and feldspar, mostly sanidine. No mafic phases remain. Silica, clay, zeolites and Fe-oxides replace all the groundmass glass and fill in the voids (Chipera et al., in press; 2007). Silica addition diminishes the total alkali contents of these rocks in a fairly linear fashion (Appendix 1; Fig. 4). The ignimbrite we sampled contains 14,000 ppm sulfur, suggesting that alunite is present as an alteration mineral because we found no sulfides. The lavas contain microphenocrysts to phenocrysts of quartz and sanidine but no mafic phases other than occasional opaque oxides. The groundmass is usually silicified, and commonly banded and spherulitic, giving many rocks a cherty appearance. Deer Canyon lavas are high-silica rhyolites, generally having more silica but approximately the same total alkali content as the Tshirege Member of the Bandelier Tuff (Appendix 1; Fig. 4). Many Deer Canyon lavas contain exceptionally low quantities of MgO and CaO (Appendix 1). Trace elements are difficult to evaluate because of alteration, but the lavas appear to have less Ba, Rb, Sr, and Zr than the Unit 4L and 4U Tshirege rocks on the resurgent dome.

The Redondo Creek Member is the final early rhyolite erupted on the resurgent dome and is dated by $^{40}Ar/^{39}Ar$ at 1.208 to 1.239 Ma (Phillips et al., in press). It consists of flows, flow breccias, and block-and-ash flows of flow-banded, porphyritic lava containing phenocrysts of plagioclase, biotite, clinopyroxene, and minor sanidine. Samples are commonly perlitic to spherulitic. It is the only rhyolite (lava or tuff) in Valles caldera that does not contain quartz, which makes it supremely useful as a stratigraphic marker. Redondo Creek lavas erupted from multiple vents. One vent and associated lava flows occupy the intersection of the major grabens cutting the resurgent dome. Other Redondo Creek lavas erupted from at least three vents on the western side of the resurgent dome and spilled into the western moat. These flow complexes may be more than 200 m thick and butted up against the western caldera wall. No doubt the thick Redondo Creek flows acted as temporary dams to the drainage system in the western moat. Redondo Creek lavas overlie Deer Canyon rocks and are interbedded with caldera- fill sediments including lacustrine deposits (described below) in the western moat (Kelley et al., 2004) and other parts of the resurgent dome. Many of the Redondo Creek lavas on the western resurgent dome display extreme hydrothermal alteration (Charles et al., 1986).

In thin section, most Redondo Creek samples show partially devitrified, banded to perlitic textures. Spherulites and tridymite are common. Few samples are completely glassy. Feldspar and biotite phenocrysts are abundant and distinct. Clinopyroxene crystals are commonly altered. Highly altered samples show extensive silicification and few if any phenocrysts are preserved. Pyrite is common in such samples. Chemically, the Redondo Creek lavas are rhyolite (not high-silica rhyolite) with slightly less silica but similar total alkalis to most samples of the Tshirege Member exposed on the resurgent dome (Fig. 4). Compared to Deer Canyon lavas, the Redondo Creek samples generally contain more total Fe oxides, more MgO, CaO and Ba but less Sr.

Early caldera-fill sedimentary rocks

Valles caldera contains a diverse assemblage of sedimentary rocks deposited early in the caldera history. These consist of a mixture of debris flows, talus breccias, landslides, fluvial, deltaic, and lacustrine deposits. Many of these sediments were deposited soon after the caldera formed but many were deposited as the resurgent dome grew. The sediments directly overlie the Tshirege Member and are interbedded with the Deer Canyon and Redondo Creek Members. Because resurgent uplift was not everywhere equal, the deposits are best preserved on the north and west flanks of the resurgent dome. The 1:24,000 geologic maps (see Fig. 2) break this unit into two parts; a dominantly coarse, debris flow unit (Qdf, Fig. 3) and a fluvial and lacustrine unit (Qvs, e.g., Goff et al., 2005a). Geothermal wells in the Redondo Creek area of the resurgent dome generally encounter a few tens of meters or less of these deposits (Nielson and Hulen, 1984), whereas wells on the northwestern resurgent dome intersect up to several hundred meters of early sediments (Lambert and Epstein, 1980; Goff and Gardner, 1994). For example, the debris flow unit is exposed at 2715 m in the pass between the Cerro Seco and San Antonio Mountain moat rhyolites (Fig. 1), indicating that the caldera-fill sedimentary sequence was once dramatically thicker in the caldera than we see today.

The matrix of debris flow deposits tends to be white to pale green or yellow, pumice and ash-rich sandstone. Other sand-sized fragments consist of chert, precaldera volcanics, probable Tertiary and Permian sandstone, Precambrian granitoids, aphyric rhyolite, Bandelier Tuff (both Otowi and Tshirege Members),

quartz, feldspar, biotite, and rare pyroxene and hornblende. Sorting is extremely poor and most fragments are angular to subangular. Cobbles and boulders in basal debris flows consist mostly of precaldera volcanics, sandstones, granitoids, and silicified tuff of the Otowi Member. Precaldera volcanics overwhelmingly dominate the coarse clastic material in upper debris flows such as those on the north side of the resurgent dome. During the mapping, we also found at least two debris flow deposits composed almost entirely of tuffs of the Tshirege Member.

Sandstones are white, gray, tan, or pale pink, massive to bedded deposits. Some sandstones are pumice and ash-rich, while others are not. Other fragments resemble those described above. Sorting and fragment rounding are highly variable. Most sandstones are moderately well sorted and have subangular to subrounded fragments. Some sandstone beds show cross bedding, graded bedding, groove features, and ripple marks.

Lacustrine rocks consist of white to gray, laminated to finely bedded mudstone and siltstone. Layers are often only fractions of a millimeter thick and superficially resemble varves. Crystal fragments are sparse to rare and consist of quartz, feldspar (mostly sanidine) and very rare pyroxene. Black organic smudges are common. Small fossil leaves are rarely found. Diatom remains are very common in the muddier lacustrine samples. Small faults and fractures are also common. The matrix is often highly silicified.

Most early caldera-fill sedimentary rocks show low-temperature hydrothermal alteration. X-ray diffraction analyses show that much of the alteration is silica, clays, zeolites, alunite, and Fe-oxides (Chipera et al., in press; 2007). Some samples show green, Fe-rich illite and/or chlorite. Quartz, chalcedony, and rarely calcite fill cavities and vugs, and cement grain boundaries. Chemically, the sedimentary deposits tend to be silica-rich and alkali-poor (Appendix 1; Fig. 4). One limonite-cemented sandstone contains over 16 wt-% Fe_2O_3. Some samples contain high sulfur, arsenic, and some heavy metals.

Veins, gouge, mineralization and other breccias

No description of the Valles resurgent dome would be complete without mention of rocks influenced by hydrothermal processes. Most major faults contain zones of veins, gouge, and breccia composed mostly of quartz, chalcedony, opal, and small quantities of sulfides, kaolin, and alunite. The breccias contain recognizable fragments of silicified tuff. These rocks are often brightly colored to orange, red, brown, and pink. The host rock is usually Tshirege Member of Bandelier Tuff. Silica is enriched and alkalis are depleted (Appendix 1; Fig. 4). Sulfur, arsenic, and iron are frequently enriched. Small sinter deposits (silica-rich hot spring deposits or geyserite) also remain on the resurgent dome adjacent to or cut by faults, but are too small to show on Figure 2. The altered rocks and sinters are the surface expressions of the hydrothermal system(s) that have circulated within the resurgent dome since caldera formation. The deeper parts of the Valles hydrothermal system and associated alteration and mineralization have been described in several papers (see Goff and Gardner, 1994, and papers cited therein).

Finally, we examined one *disaggregation* breccia (our term), a mixture of dacite tuff and comminuted Tshirege Member, Bandelier Tuff. This rock occurs at the margin of a dacite tuff collapse breccia block and the enclosing Tshirege. In thin section, it is a mixture of angular dacite tuff fragments submerged in what appears to be fluidized Bandelier Tuff, rich in crystals but poor in pumice. Dacite comprises about 70% of the rock. Chemically, this breccia plots between benmoreite and Bandelier Tuff (Appendix 1; Fig. 4). Breccias with such textures are common around the margins of many collapse breccia blocks.

CERRO SECO RHYOLITE

Cerro Seco (Fig. 1) is one of the northern moat domes of the Valles Grande Member (Bailey et al., 1969). Initial eruptions of Cerro Seco magma produced ignimbrite, hydromagmatic surge and associated sediments that formed a depositional apron in the north caldera moat around the northern sector of Cerro Seco dome (Goff et al., 2006). The pyroclastic phase was followed by growth of the rhyolite dome. Pumice and lava consist of moderately porphyritic rhyolite containing phenocrysts of quartz, sanidine, biotite, and very rare green hornblende. The sanidine is often chatoyant. The hornblende can only be seen in thin sections. Because of debate about the age and origin of the pyroclastic deposits, we analyzed a rhyolite vitrophyre block from ignimbrite a few hundred meters northwest of Cerro Seco to determine if a genetic relation exists between dome and pyroclastic phases (Appendix 1; Fig. 4). Cerro Seco eruptive products are high-silica rhyolite with total alkalis slightly higher than Deer Canyon or Redondo Creek lavas. TiO_2, Ba, and Sr contents are relatively low but Nb, Rb, and Y are somewhat high. On a LOI-free basis, the chemistry of the two Seco samples is very comparable, indicating that the ignimbrite and dome originate from the same magma.

CONCLUSIONS

Ignimbrites of the Tshirege Member (upper Bandelier Tuff) in Valles caldera are spatially extensive but significant stratigraphic sections are exposed only along graben walls within the interior of the resurgent dome. Petrographically and chemically, unaltered Tshirege exposed on the resurgent dome correlates with the uppermost Tshirege outflow sheets described on the western Pajarito Plateau south of Los Alamos (units 4 and 5 of Warren et al., 1997; units 4L and 4U of Gardner et al., 2001, and generally, units E and F of Rogers, 1995). Caldera collapse breccia blocks consist of various lithologies of Pennsylvanian to Quaternary age. They are numerous, particularly in the central and eastern resurgent dome (Fig. 2)**.** The largest collapse breccia is about 2 km long and 0.5 km wide. Early post-caldera rhyolites consist of various tuffs, lava flows, and flow breccias erupted from numerous vents on the resurgent dome. Most early rhyolite samples display moderate to extensive low- to moderate-temperature hydrothermal alteration. Early postcaldera sediments consist of debris flows, talus breccias, fluvial and lacustrine deposits formed during erosion of caldera walls, erosion of the uplifted resurgent dome, and deposition into the earliest intracaldera lake(s). These sediments

are best preserved on the lower flanks and least uplifted portions of the resurgent dome (Fig. 2). Alteration and veining are most intense along faults where gouge and breccia provide conduits for hydrothermal fluids. Altered rocks generally show silicification and enhanced Fe, S, and As contents. Pyroclastic deposits flanking the north side of Cerro Seco contain vitrophyre blocks that chemically resemble lavas from Cerro Seco dome. Thus, we believe these pyroclastic rocks and this dome formed from the same magma batch at about the same time.

ACKNOWLEDGMENTS

We thank the Valles Caldera National Preserve, the New Mexico Bureau of Geology and Mineral Resources, and Los Alamos National Laboratory for logistical and financial support. Polished thin sections were prepared by High Mesa Petrographics (David Mann), Los Alamos. The draft manuscript was reviewed by Shari Kelley and Steve Chipera.

REFERENCES

Bailey, R., Smith, R., and Ross, C., 1969, Stratigraphic nomenclature of volcanic rocks in the Jemez Mountains, New Mexico: U.S. Geological Survey, Bulletin1274-P, 19 p.

Caress, M.E., 1996, Zonation of alkali feldspar compositions in the Tshirege Member of the Bandelier Tuff in Pueblo Canyon, near Los Alamos, New Mexico: New Mexico Geological Society, 47th Field Conference, Guidebook, p. 275-283.

Charles, R., Vidale, R., and Goff, F., 1986, An interpretation of the alteration assemblages at Sulphur Springs, Valles Caldera, New Mexico. Journal of Geophysical Research, v. 91, p. 1887-1898.

Chipera, S.J., Goff, F., Goff, C.J., and Fittapaldo, M., in press, Zeolitization of intracaldera sediments and rhyolitic rocks in the 1.25 Ma lake of Valles caldera, New Mexico, USA: Journal of Volcanology and Geothermal Research.

Chipera, S., Goff, F., Goff, C.J., and Mittipaldo, M., 2007, Zeolitization of intracaldera sediments and rhyolitic rocks in the Valles caldera, New Mexico: New Mexico Geological Society, 58th Field Conference, Guidebook, p. 373-381.

Criss, J., 1979. Software Inc., 12204 Blaketon St., Largo, MD 20870.

Doell, R., Dalrymple, G., Smith, R.L., and Bailey R.A., 1968, Paleomagnetism, potassium argon ages, and geology of rhyolites and associated rocks of the Valles caldera, New Mexico: Geological Society of America, Memoir 116, p. 211-248.

Gardner, J.N. Goff, F., Garcia, S., and Hagan, R., 1986, Stratigraphic relations and lithologic variations in the Jemez volcanic field, New Mexico: Journal of Geophysical Research, v. 91, p. 1763-1778.

Gardner, J.N., Reneau, S.L., Lewis, C.J., Lavine, A., Krier, D.J., WoldeGabriel, G., and Guthrie, G.D., 2001, Geology of the Pajarito fault zone in the vicinity of S-Site (TA-16), Los Alamos National Laboratory, Rio Grande rift, New Mexico: Los Alamos National Laboratory, Report LA-13831-MS, 84 p.

Gardner, J.N., Goff, F., Reneau, S.L., Sandoval, M., Drakos, P., Katzman, D., and Goff, C.J., 2006, Preliminary geologic map of the Valle Toledo 7.5-minute quadrangle, Sandoval County, New Mexico: New Mexico Bureau of Geology and Mineral Resources, Open-file Geologic Map OF-GM-133, scale 1:24,000.

Goff, F., and Gardner, J.N., 1994, Evolution of a mineralized geothermal system, Valles caldera, New Mexico: Economic Geology, v. 89, p. 1803-1832.

Goff, F., Bergfeld, D., Janik, C.J., Counce, D., and Murrell, M., 2002, Geochemical data on waters, gases, scales, and rocks from the Dixie Valley region, Nevada (1996-1999): Los Alamos National Laboratory, Report LA-13972-MS, 71 p.

Goff, F., Gardner, J.N., Reneau, S.L., and Goff, C.J., 2005a, Preliminary geologic map of the Redondo Peak 7.5-minute quadrangle, Sandoval County, New Mexico: New Mexico Bureau of Geology and Mineral Resources, Open-file Geologic Map OF-GM-111, scale 1:24,000.

Goff, F, Reneau, S.L, Lynch, S., Goff, C.J., Gardner, J.N., Drakos, P. and Katzman, D., 2005b, Preliminary geologic map of the Bland 7.5-minute quadrangle, Los Alamos and Sandoval Counties, New Mexico: New Mexico Bureau of Geology and Mineral Resources, Open-file Geologic Map OF-GM-112, scale 1:24,000.

Goff, F., Reneau, S.L., Goff, C.J., Gardner, J.N., Drakos, P. and Katzman, D., 2006, Preliminary geologic map of the Valle San Antonio 7.5-minute quadrangle, Sandoval and Rio Arriba Counties, New Mexico: New Mexico Bureau of Geology and Mineral Resources, Open-file Geologic Map OF-GM-132, scale 1:24,000.

Govindaraju, K., 1994, Compilation of working values and sample description for 383 geostandards: Geostandards Newsletter, v. 18, p. 15-35.

Hulen, J., and Nielson, D., 1986, Hydrothermal alteration in the Baca geothermal system, Redondo dome, Valles caldera, New Mexico: Journal of Geophysical Research, v. 91, p. 1867-1886.

Hulen, J., Nielson, D., and Little, T., 1991, Evolution of the western Valles caldera complex, New Mexico: evidence from intracaldera sandstones, breccias, and surge deposits: Journal of Geophysical Research, v. 96, p. 8127-8142.

Izett, G.A., and Obradovich, J.D., 1994, $^{40}Ar/^{39}Ar$ age constraints for the Jaramillo normal subchron and the Matuyama-Brunhes geomagnetic boundary: Journal of Geophysical Research, v. 99, p. 2925-2934.

Kelley, S., Kempter, K.A., Goff, F., Rampey, M., Osburn, G.R., and Ferguson, C.A., 2003, Preliminary geologic map of the Jemez Springs 7.5-minute quadrangle, Sandoval County, New Mexico: New Mexico Bureau of Geology and Mineral Resources, Open-file Geologic Map OF-GM-73, scale 1:24,000.

Kelley, S., Osburn, G.R., Ferguson, C., Kempter, K., and Osburn, M., 2004, Preliminary geologic map of the Seven Springs 7.5-minute quadrangle, Sandoval County, New Mexico: New Mexico Bureau of Geology and Mineral Resources, Open-file Geologic Map OF-GM-88, scale 1:24,000.

Kues, B.S. and Goff, F., 2007, Pennsylvanian paleontology of limestone blocks in the resurgent dome of Valles caldera: New Mexico Geological Society, 58th Field Conference, Guidebook, p. 85-87.

Lambert, S.J., and Epstein, S., 1980. Stable isotope investigations of an active geothermal system in the Valles caldera, Jemez Mountains, New Mexico: Journal of Volcanology and Geothermal Research, v. 8, p. 111-129.

Le Bas, M.J., Le Maitre, R.W., Streckeisen, A., and Zanettin, B., 1986, A chemical classification of volcanic rocks based on the total alkali-silica diagram: Journal of Petrology, v. 27, p. 745-750.

Lewis, C.J., Lavine, A., Reneau, S.L., Gardner, J.N., Channell, R., and Criswell, W.C., 2002, Geology of the western part of Los Alamos National Laboratory (TA-3 to TA-16), Rio Grande rift, New Mexico: Los Alamos National Laboratory, Report LA-13960-MS, 98 p.

Lipman, P.W., 1976, Caldera collapse breccias in the southern San Juan Mountains, Colorado: Geological Society of America Bulletin, v. 87, p. 1397-1410.

Lipman, P.W., 2000, Calderas, *in* Sigurdsson, H., Houghton, B., McNutt, S., Rymer, H., and Stix, J., eds., Encyclopedia of volcanoes: San Diego, Academic Press, p. 643-662.

Nielson, D., and Hulen, J., 1984, Internal geology and evolution of the Redondo dome, Valles caldera, New Mexico: Journal of Geophysical Research, v. 89, p. 8695-8711.

Nowell, D., 1996, Gravity modeling of the Valles caldera: New Mexico Geological Society, 47th Field Conference, Guidebook, p. 121-128.

Phillips, E.H., 2004, Collapse and resurgence of the Valles caldera, Jemez Mountains, New Mexico: $^{40}Ar/^{39}Ar$ age constraints on the timing and duration of resurgence and ages of megabreccia blocks [M.S. thesis]: Socorro, New Mexico Institute of Mining and Technology, 200 p.

Phillips, E.H., Goff, F., Kyle, P.R., McIntosh, W.C., Dunbar, N.W., and Gardner, J.N., in press, $^{40}Ar/^{39}Ar$ age constraints on the duration of resurgence at the Valles Caldera, New Mexico: Journal of Geophysical Research.

Rogers, J.B., Smith, G.A., and Rowe, H., 1996, History of formation and drainage of Pleistocene lakes in the Valles caldera: New Mexico Geological Society, 47th Field Conference, Guidebook, p. 14-16.

Rogers, M.A., 1995, Geologic map of the Los Alamos National Laboratory Reservation, State of New Mexico Environmental Department, scale 1:4800.

Ross, C.S., and Smith, R.L., 1961, Ash-flow tuffs: their origin, geologic relations and identification: U.S. Geological Survey, Professional Paper 366, 81 p.

Self, S., Kircher, D.E., and Wolff, J.A., 1988, The El Cajete Series, Valles caldera,

New Mexico: Journal of Geophysical Research, v. 93, p. 6113-6127.
Smith, R.L., and Bailey, R.A., 1966, The Bandelier Tuff: a study of ash-flow eruption cycles from zoned magma chambers: Bulletin of Volcanology, v. 29, p. 83-104.
Smith, R.L., and Bailey, R.A., 1968, Resurgent cauldrons: Geological Society of America, Memoir 116, p. 613-662.
Smith, R. Bailey, R., and Ross, C., 1970, Geologic map of the Jemez Mountains, New Mexico: U.S. Geological Survey, Miscellaneous Geologic Investigations Map I-571, scale 1:125,000.
Spell, T.L., and Kyle, P.R., 1989, Petrogenesis of Valle Grande Member rhyolites, Valles caldera, New Mexico: implications for evolution of the Jemez Mountains magmatic system: Journal of Geophysical Research, v. 94, p. 10,379-10,396.
Spell, T.L., McDougall, I., and Doulgeris, A.P., 1996, Cerro Toledo Rhyolite, Jemez Volcanic Field, New Mexico: $^{40}Ar/^{39}Ar$ geochronology of eruptions between two caldera-forming events: Geological Society of America Bulletin, v. 108, p. 1549-1566.
Warren, R.G., McDonald, E.V., and Ryti, R.T., 1997, Baseline geochemistry of soil and bedrock Tshirege Member of the Bandelier Tuff at MDA-P: Los Alamos National Laboratory, Report LA-13330-MS, 89 p.
Warren, R.G., Goff, F., Kluk, E.C., and Budahn, J.R., 2007, Petrography, chemistry, and mineral compositions for subunits of the Tshirege Member, Bandelier Tuff within the Valles caldera and Pajarito Plateau: New Mexico Geological Society, 58th Field Conference, Guidebook, p. 316-332.
WoldeGabriel, G., and Goff, F., 1992, K/Ar dates of hydrothermal clays from corehole VC-2B, Valles caldera, New Mexico and their relation to alteration in a large hydrothermal system: Journal of Volcanology and Geothermal Research, v. 50, p. 207-230.
WoldeGabriel, G., Warren, R.G., Broxton, D.E., Vaniman, D.T., Heizler, M.T., Kluk, E.C., and Peters, L., 2001, Episodic volcanism, petrology, and lithostratigraphy of the Pajarito Plateau and adjacent areas of the Española Basin and the Jemez Mountains*:* New Mexico Museum of Natural History and Science, Bulletin 18, p. 97-129.
Wolff, J.A., Rowe, M.C., Teasdale, R., Gardner, J.N., Ramos, F.C., and Heikoop, C.E., 2005, Petrogenesis of pre-caldera mafic lavas, Jemez Mountains volcanic field (New Mexico, USA): Journal of Petrology, v. 46, p. 407-439.

APPENDIX 1. Chemical analyses of rocks from the resurgent dome and vicinity of Valles caldera, and comparisons with similar units in the Jemez Mountains, New Mexico. Location numbers are shown on Plate X (na = not analyzed, nd = not detected, mbx = megabreccia, ss = sandstone).

Unit/Rock	**Tshirege**	**Tshirege**	**Tshirege**	**Tshirege**	**Tshirege**	**Tshirege**	**Tshirege**	**Tshirege**	**Tshirege**	**Tshirege**	**Tshirege**	**Tshirege**	**Tshirege**	**Tshirege**	**Tshirege**	**Tshirege**
Sample	F02-14	F02-25	F02-31	F02-33	F02-35	F02-54	F02-57	F03-40[a]	F03-41	F03-42	F03-45	F03-43	F03-44	F03-46	Unit 4L[b]	Unit 4U[c]
Description	Welded	Welded	Welded	Vitrophyre	Welded	Welded	Glassy	Vesicular	Vitrophyre	Welded	Welded	Welded	Welded	Welded	Ave of 7	Ave of 5
Plate No.	1	2	3	4	5	6	7	8 (9610 ft)	8	8	8 (9475 ft)	8 (9475 ft)	8 (9405 ft)	8 (9350 ft)	Paj. Plateau	Paj. Plateau
Lat (+35°)	53.496'	53.205'	53.122'	53.205'	53.351'	54.502'	54.129'	53.312'	1.5 m	3.0 m	1 m above	1 m below				
Long (+106°)	29.864'	32.653'	32.959'	32.653'	31.747'	30.523'	32.666'	35.448'	below 40	below 41	contact	contact				
Major Elements (wt%)																
SiO_2	72.66	74.74	73.29	71.97	73.21	72.97	70.00	81.67	71.43	74.66	76.91	74.88	68.63	70.74	71.58	72.26
TiO_2	0.264	0.221	0.250	0.219	0.237	0.243	0.258	0.182	0.230	0.220	0.321	0.336	0.425	0.390	0.314	0.242
Al_2O_3	13.34	13.06	13.61	13.15	13.50	13.83	13.29	9.46	12.69	12.43	11.62	12.77	15.79	14.53	13.74	13.52
Fe_2O_3	2.18	1.37	1.80	1.26	1.98	1.99	1.42	0.96	1.34	1.61	1.15	1.50	2.20	2.38	2.60	2.25
FeO	0.20	0.30	0.25	0.74	0.29	0.17	0.25	0.19	0.59	0.17	0.09	0.12	0.20	0.21	na	na
MnO	0.096	0.018	0.021	0.083	0.074	0.013	0.019	0.025	0.081	0.030	0.014	0.019	0.015	0.017	0.083	0.059
MgO	0.11	<0.06	<0.06	0.17	<0.06	0.08	0.32	0.10	0.17	0.07	0.13	0.10	0.13	0.16	0.030	0.15
CaO	0.44	0.34	0.38	0.71	0.36	0.38	1.19	0.35	1.25	0.53	0.70	0.68	0.88	0.72	0.87	0.47
Na_2O	4.30	4.17	4.51	4.36	4.54	4.36	2.57	2.21	4.26	3.53	3.09	3.42	4.61	4.47	4.66	4.13
K_2O	4.78	4.95	4.82	4.66	4.82	4.68	4.45	3.92	3.17	4.89	3.95	4.24	5.35	4.71	4.52	4.79
P_2O_5	0.057	0.035	0.049	0.045	0.040	0.021	0.047	0.035	0.034	0.061	0.055	0.060	0.081	0.082	0.063	0.037
LOI	0.90	0.49	1.04	2.30	0.64	0.98	5.16	0.93	4.09	1.41	1.09	1.25	1.18	1.02	0.57	1.93
Trace Elements (ppm, XRF)																
Ba	420	230	342	287	313	316	1130	408	301	357	740	559	747	553	465	312
Cr	<8	<8	<8	12.0	<8	<8	<8	<8	<8	<8	<8	<8	<8	9.2	nd	<8
Nb	33.5	46.1	40.0	49.4	47.2	32.6	39.5	24.0	45.0	50.1	40.4	31.2	42.6	37.4	36.7	43.2
Ni	<11	<12	<12	<12	<12	<11	<11	<12	<12	<12	<12	<12	<12	<12	nd	<11
Rb	83.1	96.2	85.2	93.1	84.4	82.1	102	63.1	215	102	81.0	74.9	95.5	81.4	82.4	84.3
Sr	64.6	52.9	59.2	60.4	61.9	59.8	332	67.6	149	64.6	124	116	147	131	111	51.2
V	<10	12.1	11.8	<10	17.9	<10	15.2	11.7	<10	15.8	12.2	13.8	22.0	29.7	nd	<10
Y	26.7	27.3	29.8	34.6	25.1	28.5	29.6	28.6	34.0	31.8	12.5	18.6	32.9	31.2	35.6	32.2
Zn	106	61.6	77.6	78.2	72.4	48.8	68.8	86.8	71.5	56.2	26.3	53.9	63.7	90.0	71.4	73.2
Zr	403	348	389	348	378	403	342	233	333	352	320	341	435	404	373	381
Total (wt%)	99.47	99.81	100.15	99.79	99.82	99.83	99.22	100.15	99.47	99.72	99.28	99.51	99.68	99.59	99.15	99.90
Trace Elements (ppm, wet methods)																
As	1.73	0.39	0.62	0.98	0.93	0.92	0.49	2.53	0.80	4.81	27.8	6.50	18.3	2.41	na	0.93
B	5.72	5.79	5.00	5.06	4.70	5.51	5.16	8.82	5.33	7.61	3.13	4.27	3.72	5.08	na	6.21
Br	<2	<2	4.66	6.62	<2	8.77	<2	0.41	0.81	0.81	0.61	0.62	0.63	0.62	na	2.53
Cl	191	43.7	296	646	76.4	124	48.2	248	586	250	157	235	171	171	na	298
Cr	2.66	3.72	2.17	2.95	2.57	2.12	3.44	na	na	na	na	na	na	na	na	2.88
Cs	2.10	0.88	2.77	5.88	2.77	1.74	17.5	2.55	108	2.31	2.13	2.25	1.35	1.54	na	1.50
F	321	89.2	193	434	206	273	645	407	225	30.7	258	124	174	282	na	446
Li	17.2	23.5	10.8	19.6	11.7	8.72	16.7	151	26.5	63.0	90.3	82.5	34.6	37.1	na	18.6
Mo	2.86	2.69	3.26	5.69	2.35	1.86	1.83	1.20	3.91	2.93	1.02	1.14	1.28	2.16	na	4.88
P_2O_5	712	564	757	597	593	300	563	491	498	807	715	745	1030	1050	na	463
Rb	86.3	104	94.0	106	97.8	103	119	123	235	145	129	122	147	131	82.4	98.4
S	60.7	46.9	50.0	61.9	40.0	43.8	43.1	89	105	282	81	82	110	41	na	58.5

[a]Samples F03-40 through F03-46 comprise a section exposed along the east side of Redondo Border (see Fig. 1).

[b]Samples of Tshirege Member, Bandelier Tuff, lower Unit 4 as described by Lewis et al. (2002).

[c]Samples of Tshirege Member, Bandelier Tuff, upper Unit 4 exposed near NM Highway 4 about 1.5 miles east of junction with NM Highway 502. Criteria for identification follow Gardner et al. (2001) and Lewis et al. (2002).

APPENDIX 1. Continued.

Unit/Rock	Otowi	Otowi	Otowi	Otowi	Dacite	Dacite	Dacite	Dacite Tuff	Andesite	Andesite	Andesite	Abiquiu	Santa Fe	Permian	Permian
Sample	F02-30	F02-36[d]	F02-84	Section[e]	F02-56	F02-58	JG80-12[f]	F02-66	F02-67	F03-06	JG81-4B[g]	F02-79	F03-39	F02-92	F03-05
Description	Boulder	Mbx	Mbx	Ave of 9	Mbx	Mbx	Tschicoma	Mbx	Mbx	Mbx	Pal. Can.	SS, Mbx	SS, Mbx	SS Block	SS, Mbx
Plate No.	9	10	11	Paj. Plateau	12	13		14	15	16		17	18	19	20
Lat (+35°)	53.828'	54.305'	55.280'		54.601'	54.181'		55.425'	55.301'	55.133'		55.405'	54.356'	53.589'	55.061'
Long (+106°)	30.969'	30.204'	33.929'		31.842'	32.704'		33.240'	33.214'	34.129'		33.674'	35.532'	33.393'	33.984'
Major Elements (wt%)															
SiO_2	77.64	75.71	80.57	75.43	65.10	64.86	67.21	62.94	60.80	63.11	63.47	88.17	96.92	87.08	88.37
TiO_2	0.164	0.166	0.112	0.14	0.764	0.624	0.51	0.658	0.858	0.889	0.83	0.101	0.036	0.129	0.142
Al_2O_3	11.69	12.70	9.94	12.22	15.68	15.57	15.28	15.61	15.47	16.62	16.75	5.91	1.63	5.80	5.68
Fe_2O_3	1.39	1.41	0.86	1.66	4.36	1.98	3.68	3.09	4.52	3.72	4.45	0.37	0.16	0.88	0.38
FeO	0.12	0.15	0.11	na	0.25	1.21	na	0.48	1.09	1.09	na	0.10	<0.01	0.13	0.08
MnO	0.013	0.031	<0.009	0.07	0.027	0.061	0.06	0.028	0.106	0.084	0.09	0.029	0.047	<0.009	<0.009
MgO	<0.06	<0.06	0.11	0.14	0.51	1.61	1.69	1.25	1.20	1.01	1.65	0.29	0.19	0.14	0.14
CaO	0.19	0.24	0.17	0.49	3.25	3.43	3.40	4.13	5.78	4.63	3.87	0.22	0.13	0.12	<0.12
Na_2O	3.91	3.98	2.71	3.68	3.80	3.82	3.90	2.30	3.71	4.12	4.23	<0.12	<0.12	0.52	0.63
K_2O	4.45	4.88	4.23	4.75	3.38	2.71	3.18	2.87	3.70	3.11	3.18	2.27	0.53	3.72	3.51
P_2O_5	0.024	<0.009	0.012	0.022	0.257	0.210	0.140	0.212	0.319	0.303	0.25	0.018	<0.009	0.013	0.010
LOI	0.37	0.61	0.83	1.69	2.07	3.53	1.46	5.89	1.70	0.64	1.33	1.93	0.85	0.90	0.64
Trace Elements (ppm, XRF)															
Ba	175	<43	146	156	1200	1350	1180	1790	1200	1270	1440	610	103	632	538
Cr	<8	<8	<8	nd	18.2	28.3	22	27.2	26.0	41.6	11	<8	<8	<8	<8
Nb	48.2	45.0	71.8	93	16.2	27.5	17.3	27.4	19.3	26.5	25	8.7	<7	<7	<8
Ni	<12	<12	<12	nd	30.6	<12	na	18.9	30.0	16.0	na	<12	<12	<12	<12
Rb	91.2	97.0	170	200	76.5	179	79	74.9	109	68.1	68	67.6	16.2	92.6	83.2
Sr	26.5	13.4	27.0	53	570	579	510	900	662	699	769	37.3	13.3	52.2	49.8
V	<10	<10	11.0	nd	88.7	146	58	69.3	127	106	78	61.1	<10	21.7	15.8
Y	45.1	15.8	51.2	56	20.8	15.1	na	<7	37.6	24.6	na	11.0	<7	14.1	34.7
Zn	92.1	44.6	29.4	82	74.0	58.3	na	47.5	76.7	61.5	52	<12	<12	18.2	<12
Zr	306	328	150	210	211	243	189	241	226	223	360	57.6	32.2	73.7	223
Total (wt%)	100.05	99.94	99.73	100.36	99.72	99.90	100.51	99.84	99.77	99.62	100.10	99.50	100.20	99.53	99.67
Trace Elements (ppm, wet methods)															
As	3.41	2.48	2.22	na	1.54	1.09	na	0.60	0.99	1.17	na	1.37	0.50	1.40	1.09
B	6.98	4.64	4.63	na	6.52	9.77	na	4.80	5.92	12.4	na	6.48	3.79	7.72	11.2
Br	4.53	<2	<2	na	<2	4.45	na	<2	<2	<0.4	na	2.47	<0.4	<2	0.60
Cl	166	222	33.7	na	31.1	406	500	83.9	43.8	266	620	83.1	213	49.6	340
Cr	3.59	2.95	6.53	na	17.4	15.4	22	18.3	18.0	na	11	5.84	na	7.92	na
Cs	2.35	1.93	1.54	na	1.83	12.1	1.4	1.87	1.40	1.23	2.2	1.74	<0.4	1.70	129
F	88.8	137	378	na	425	412	na	410	458	385	na	99.4	71.9	85.3	50.5
Li	11.6	16.4	53.5	na	11.6	7.96	na	11.4	9.54	14.7	na	12.3	17.6	17.4	25.0
Mo	4.02	2.11	1.03	na	1.78	2.70	na	0.50	1.59	2.34	na	0.54	0.01	1.02	0.43
P_2O_5	370	164	150	na	2800	2310	na	2410	3330	3180	na	196	116	132	199
Rb	103	109	188	200	99.1	185	79	87.3	113	121	68	89.4	71.3	97.4	130
S	47.3	56.3	52.7	na	206	68.7	na	48.8	53.2	87	na	72.1	70	104	144

[d]A sample of this megabreccia was dated at 1.68 Ma (Phillips, 2004).

[e]Samples taken from SHB-3 drill hole (Gardner et al., 2001).

[f]Example of Tschicoma dacite (Gardner et al., 1986).

[g]Example of Paliza Canyon andesite (Gardner et al, 1986).

APPENDIX 1. Continued.

Unit/Rock	Red Ck.	Red Ck.	Red Ck.,	Red Ck.	Red Ck.,	Red Ck.	Deer Can.	Deer Can.	Deer Can.	Deer Can.	Deer Can.	Deer Can.	Deer Can.	Deer Can.	Deer Can.	Deer Can.	Deer Ca
Sample	F02-47	F02-48	F02-64	F02-65	F03-52	F03-53	F02-19	F02-46	F02-51	F02-52	F02-55	F02-60	F02-75	F02-87	F02-97	F03-14b	F03-49
Description	Lava	Lava	Lava	Lava	Lava	Lava	Lithic Tuff	Lithic Tuff	Dike	Lava	Lava	Alt. Ignim.	Porph. Lava	Porph. Lava	Pumice	Alt. Lava	Dike
Plate No.	21	21	22	23	24	25	26	27	28	29	30	31	32	33	west of map	34	35
Lat (+35°)	53.849'	53.849'	56.577'	56.058'	54.810'	54.006'	53.994'	54.647'	54.948'	53.973'	53.309'	56.390'	52.656'	52.562'	52.500'	52.149'	50.965
Long (+106°)	33.138'	33.138'	35.663'	34.821'	35.458'	33.793'	30.363'	31.773'	31.148'	30.510'	29.541'	31.250'	36.301'	36.480'	38.495'	36.311'	32.398
Major Elements (wt%)																	
SiO_2	84.48	69.63	72.91	72.44	72.50	70.52	70.85	73.02	77.03	77.86	74.36	70.30	78.36	78.26	75.31	72.57	72.
TiO_2	0.187	0.344	0.289	0.315	0.366	0.338	0.133	0.214	0.070	0.068	0.298	0.086	0.142	0.113	0.085	0.108	0.2
Al_2O_3	8.29	12.98	13.84	14.03	14.38	13.44	12.64	12.77	11.75	11.44	13.38	12.96	11.46	11.29	11.96	11.28	13.
Fe_2O_3	0.27	1.34	1.65	1.75	1.71	1.24	1.12	1.51	0.72	1.01	1.92	0.46	0.68	1.09	0.54	1.00	2.
FeO	0.19	0.68	0.17	0.21	0.40	0.85	0.25	<0.01	0.18	0.10	0.08	0.21	0.09	0.15	0.27	0.22	<0.
MnO	<0.009	0.054	0.034	0.038	0.040	0.053	0.086	0.093	0.037	0.044	0.026	0.024	<0.009	0.016	0.051	<0.009	0.0
MgO	0.10	0.37	0.20	0.22	0.30	0.36	0.35	0.34	<0.06	<0.06	0.13	<0.06	<0.06	<0.06	<0.06	0.26	0.
CaO	0.48	1.02	0.70	0.78	1.00	1.02	0.88	1.14	<0.12	<0.12	1.24	0.14	0.17	0.14	0.36	2.21	0.
Na_2O	2.34	2.03	4.13	4.11	4.41	3.73	1.47	1.33	3.98	3.86	3.68	0.27	3.56	3.89	2.95	1.98	4.
K_2O	3.14	6.06	4.91	4.90	4.80	4.85	4.63	3.73	4.79	4.32	4.45	2.66	4.52	4.50	5.27	2.54	4.
P_2O_5	0.039	0.069	0.020	0.039	0.078	0.063	0.011	0.033	<0.008	<0.008	0.074	0.011	<0.009	<0.009	<0.008	0.011	0.0
LOI	0.80	4.70	0.51	0.69	0.29	2.91	6.97	6.19	0.45	0.37	0.60	12.50	0.44	0.30	2.47	7.18	0.
Trace Elements (ppm, XRF)																	
Ba	361	653	695	735	757	702	204	486	<44	<44	536	<45	112	118	<43	113	4
Cr	11.3	<8	<8	<8	<8	<8	<8	9.6	<8	<8	<8	10.8	<8	<8	<8	<8	.
Nb	14.4	36.0	34.1	42.3	38.3	38.0	56.5	60.0	85.1	89.7	38.9	45.1	48.3	54.5	73.7	43.3	42
Ni	<11	<12	<12	<11	<12	<12	12.9	<12	<12	<12	<12	<12	<12	<11	<11	<12	<
Rb	67.5	158	105	90.4	111	108	200	122	207	189	135	79.5	113	105	233	103	85
Sr	61.0	102	91.2	90.4	132	105	224	312	<7	<7	175	20.1	23.0	15.3	<7	115	73
V	20.6	32.9	19.5	71.6	23.2	<10	16.2	<10	<10	<10	27.5	<10	<10	<10	<10	<10	<
Y	24.2	31.9	26.9	32.3	38.2	29.1	66.4	52.5	57.9	24.6	20.9	26.6	27.7	25.9	65.3	24.3	34
Zn	13.3	63.3	42.7	44.8	52.8	58.4	64.7	73.9	54.1	53.1	31.7	25.8	57.9	61.2	40.4	85.0	72
Zr	148	293	239	257	298	274	203	188	157	135	124	149	263	250	116	227	3
Total (wt%)	100.41	99.53	99.50	99.68	100.43	99.53	99.52	100.53	99.07	99.13	100.38	99.66	99.50	99.82	99.35	99.43	99.
Trace Elements (ppm, wet methods)																	
As	0.86	1.58	1.21	1.05	1.60	1.34	2.24	1.22	5.41	4.45	2.23	1.37	3.42	2.46	6.75	0.31	2.
B	5.15	8.07	4.96	7.02	11.7	9.77	6.57	4.59	11.8	9.77	9.73	6.14	4.22	5.25	13.1	9.08	2.
Br	6.47	8.57	<2	<2	1.23	1.35	6.45	<2	5.37	<2	<2	2.50	<2	2.50	9.02	0.63	0.
Cl	66.8	526	251	174	479	579	592	30.1	662	272	38.5	378	66.3	99.4	1220	318	1
Cr	2.68	3.31	3.45	1.91	na	na	3.49	6.47	2.50	2.39	15.5	2.63	5.70	3.72	4.79	na	
Cs	1.16	4.11	1.90	1.59	3.41	3.27	66.2	12.7	4.50	4.05	3.61	2.73	2.96	6.25	7.54	25.0	1.
F	152	379	287	296	381	458	947	503	371	191	272	276	89.3	50.3	623	212	51
Li	7.01	3.59	13.7	11.4	19.1	25.5	21.2	6.94	13.8	15.1	11.0	3.91	15.6	9.76	33.2	18.4	15
Mo	3.30	6.41	3.88	2.63	2.68	5.22	6.16	1.42	6.76	4.13	1.46	3.94	2.74	2.84	7.84	0.99	0.
P_2O_5	493	809	260	458	889	802	140	425	60	54	825	138	128	146	46	227	3
Rb	82.3	167	126	113	165	161	196	145	207	196	157	104	124	123	233	147	1
S	90.1	53.2	51.9	50.5	78	52	61.0	216	46.8	40.6	47.2	13900	26.1	37.2	52.4	1240	

APPENDIX 1. Continued.

Unit/Rock	Debris Flow	Debris Flov	Lacustrine	Lacustrine	Lacustrine	Moat Lacus	Debris Flow	Tshirege	Tshirege	Tshirege	Tshirege	Dacite Tuff	Tshirege	Tshirege	Cerro Seco	Cerro Seco
Sample	F02-13	F02-53	F02-78	F02-98	F03-25a	F03-33b	F03-51	F02-37	F02-41	F02-50	F02-68	F02-71[h]	F02-103	F02-105	F02-74[i]	S-3[j]
Description	Altered SS	Tuffac. SS	Fe-rich SS	Lacus. beds	Siltstone	Siltstone	Tuffac. SS	Chal. Vein	Opal vein	Flt Gouge	Altered	Breccia	Breccia	Breccia	Vitrophyre	Lava
Plate No.	36	37	38	W of map	39	N of map	N of map	40	41	42	43	44	45	46	N of map	N of map
Lat (+35°)	54.149'	54.139'	55.612'	52.500'	55.903'	57.662'	57.265'	53.786'	54.533'	54.948'	54.917'	54.907'	54.575'	50.965'	57.697'	
Long (+106°)	29.783'	29.656'	35.434'	38.495'	34.413'	31.302'	31.427'	31.454'	30.306'	31.174'	33.316'	33.597'	33.725'	35.319'	35.497'	
Major Elements (wt%)																
SiO_2	83.51	72.53	73.47	87.94	76.10	71.22	72.25	96.46	93.75	76.61	70.73	66.26	69.39	73.03	74.64	76.3
TiO_2	0.115	0.183	1.494	0.133	0.487	0.529	0.566	<0.013	0.213	0.062	0.226	0.879	0.171	0.399	0.027	0.09
Al_2O_3	7.70	12.37	3.40	4.18	11.30	13.88	12.81	<0.38	0.60	10.93	13.71	14.90	11.72	15.98	12.12	13.05
Fe_2O_3	1.06	1.84	16.44	1.11	3.62	2.49	2.87	2.00	2.11	1.63	0.22	4.72	1.85	3.08	0.36	0.77
FeO	0.14	0.07	0.12	0.13	0.06	0.23	0.27	0.15	0.08	0.21	0.15	0.57	0.10	0.11	0.46	na
MnO	0.016	0.077	<0.009	<0.009	<0.009	0.020	0.021	0.040	<0.009	0.014	<0.009	0.053	<0.009	<0.009	0.074	0.08
MgO	0.10	0.26	<0.06	0.71	0.08	0.68	0.65	<0.06	0.07	0.21	<0.06	0.34	<0.06	<0.06	<0.06	0.10
CaO	0.20	1.09	<0.12	0.64	0.14	0.68	0.78	<0.12	0.13	0.29	<0.12	2.80	<0.12	<0.12	0.35	0.38
Na_2O	1.68	2.69	<0.12	0.28	0.24	1.75	1.68	<0.12	<0.12	1.64	<0.12	3.77	<0.12	<0.12	3.89	4.38
K_2O	4.36	4.35	<0.04	1.02	0.67	2.77	2.73	<0.04	0.10	5.40	1.93	4.13	2.42	0.09	4.86	4.84
P_2O_5	0.030	0.010	0.137	0.029	0.175	0.680	0.110	<0.008	<0.008	0.069	0.051	0.410	0.049	0.083	<0.008	0.01
LOI	0.57	4.15	4.29	3.79	6.76	5.14	4.50	1.01	3.59	2.86	12.13	0.69	13.45	6.58	2.28	1.81
Trace Elements (ppm, XRF)																
Ba	187	153	213	693	403	480	425	<45	73	245	191	1040	472	799	<43	20
Cr	<8	<8	<8	11.4	18.9	23.3	35.8	<8	<8	<8	<8	<8	<8	<8	<8	<2.4
Nb	25.9	66.5	64.9	12.6	49.0	49.9	49.6	15.8	80.0	79.0	44.5	19.5	35.6	34.2	90.0	91.4
Ni	<12	<12	<11	<12	<12	<12	<12	<12	13.6	<11	<11	<12	<11	<11	<11	na
Rb	109	182	<9	45.8	17.5	141	150	<10	<10	182	<10	70.7	<9	<9	274	273
Sr	30.8	130	235	94.5	859	127	112	<7	9.3	22.9	45.4	520	59.9	94.4	<7	3.6
V	<10	20.1	40.6	13.9	40.9	54.6	46.7	<10	<10	31.9	14.9	103	11.7	27.7	<10	na
Y	57.3	37.5	26.4	20.2	14.9	75.4	60.5	11.3	9.4	65.1	18.8	26.0	26.6	24.1	72.9	81.0
Zn	46.5	68.3	<12	23.8	<12	114	63.4	<12	<12	61.7	<12	51.1	<12	<12	44.3	35
Zr	107	199	493	99	217	262	370	<11	89.3	201	371	284	274	405	112	119
Total (wt%)	99.54	99.73	99.50	100.07	99.82	99.61	99.32	99.66	100.68	100.04	99.24	99.77	99.25	99.52	99.17	100.00
Trace Elements (ppm, wet methods)																
As	1.35	1.51	14.6	19.1	5.96	3.39	3.57	7.78	8.55	12.7	5.34	5.08	13.5	264	3.87	3.4
B	4.71	8.18	3.02	28.50	6.79	20.1	23.5	6.07	3.31	7.09	4.33	4.13	3.60	7.58	13.1	na
Br	<2	<2	<2	0.58	<0.4	0.75	2.26	<2	<2	<2	<2	<2	<2	<2	9.07	1.20
Cl	35.2	116	38.5	230	196	364	341	135	271	171	<4	40.1	<4	11.8	1200	na
Cr	7.15	5.99	3.76	12.6	na	na	na	5.23	2.90	2.58	3.24	7.85	3.81	7.15	1.71	<2.4
Cs	1.88	19.2	<0.5	13.8	0.97	8.87	5.67	<0.5	1.15	2.40	0.88	1.35	1.06	0.77	8.90	9.7
F	319	307	160	908	230	514	401	73.2	274	437	69.2	502	157	1270	955	na
Li	104	21.3	2.23	94.2	5.43	39.8	35.8	14.5	4.17	11.7	4.42	44.8	1.83	3.83	55.0	na
Mo	0.94	2.65	19.4	1.10	5.09	2.88	1.10	4.81	3.93	1.55	1.56	1.09	3.81	248	5.91	6.5
P_2O_5	357	133	1490	374	1910	803	264	33	106	774	595	4400	537	952	58	na
Rb	109	198	24.7	92.8	77.6	169	199	30.1	31.4	197	26.8	85.7	31.1	26.8	317	273
S	52.9	130	712	135	4790	629	183	39.8	588	84.6	26300	59.3	34100	933	34.4	na

[h]Disaggregation breccia at contact between dacite tuff collapse breccia and enclosing Bandelier Tuff.

[i]Block in massive ignimbrite on northwest margin of Cerro Seco rhyolite dome.

[j]Analysis from Spell and Kyle (1989). Exact location unknown.

PLATE 13: GEOLOGIC MAP OF THE RESURGENT DOME OF THE VALLES CALDERA AND SURROUNDING CALDERA MOAT

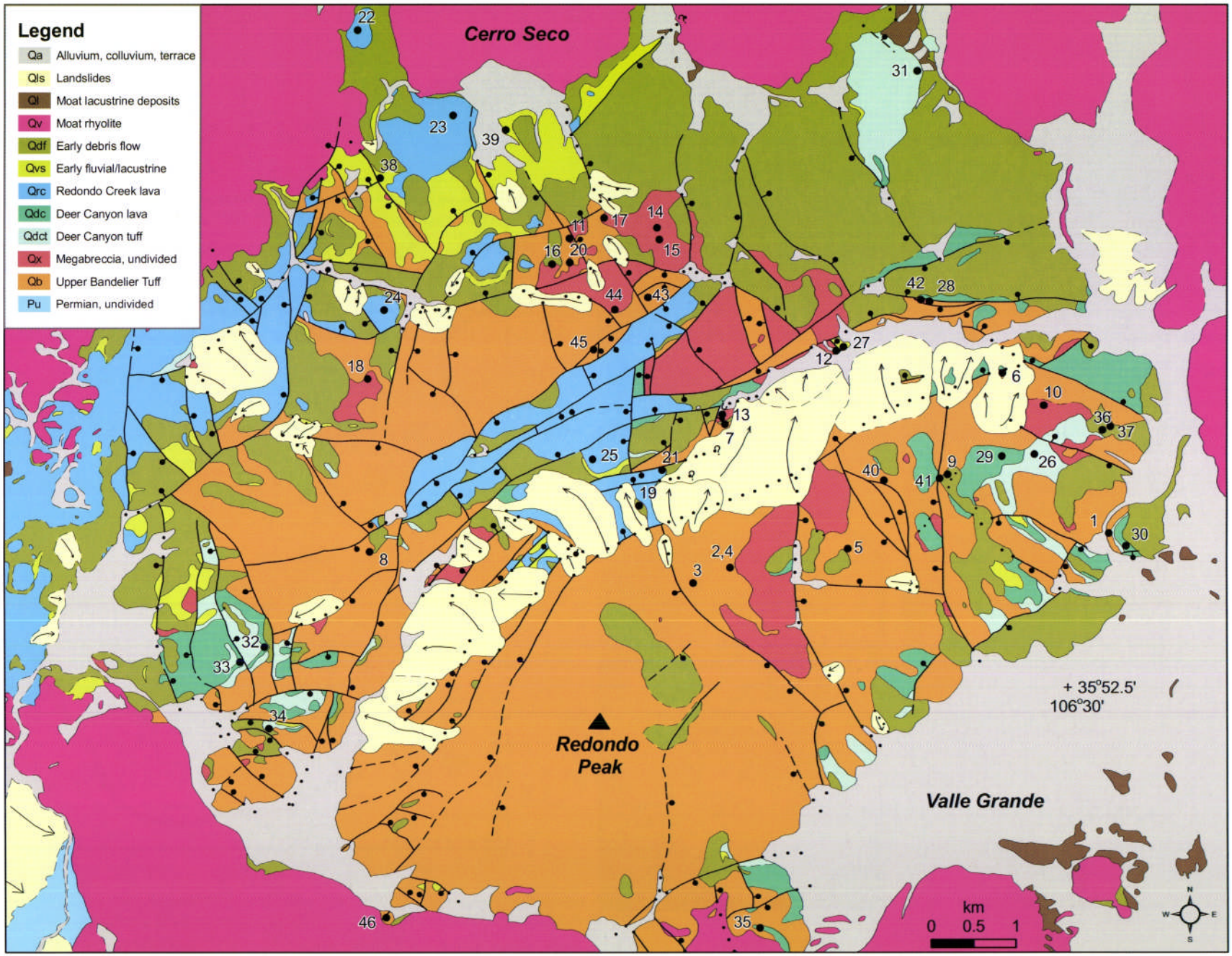

Generalized geologic map of the resurgent dome of Valles caldera and surrounding caldera moat, compiled and simplified from the following 1:24,000 maps: Bland (Goff et al., 2005b), Jemez Springs (Kelley et al., 2003), Redondo Peak (Goff et al., 2005a), Seven Springs (Kelley et al., 2004), Valle San Antonio (Goff et al., 2006), and Valle Toledo (Gardner et al., 2006). Numbers on map are keyed to sample locations in Table 1. Arrows on landslides indicate direction of movement. Ball and bar on faults indicates down-thrown side. See article by Goff et al., p. 354.